Phytochemistry 178 (2020) 112458

Contents lists available at ScienceDirect

Phytochemistry

journal homepage: www.elsevier.com/locate/phytochem

Tropane alkaloids from the stem bark of Erythroxylum bezerrae

Luana San de O. Brito [a], Francisco das Chagas L. Pinto [a], Manoel Odorico M. de Filho [b], Danilo D. Rocha [b], Maria Fernanda M. Mendoza [b], Alejandro Pedro Ayala [c], Beatriz Pinheiro Bezerra [c], Maria Iracema B. Loiola [d], Kirley M. Canuto [e], Edilberto R. Silveira [a], Otilia Deusdenia L. Pessoa [a,*]

[a] Departamento de Química Orgânica e Inorgânica, Centro de Ciências, Universidade Federal do Ceará, 60440-900, Fortaleza, CE, Brazil
[b] Departamento de Fisiologia e Farmacologia, Universidade Federal do Ceará, 60165-081, Fortaleza, CE, Brazil
[c] Departamento de Física, Universidade Federal do Ceará, 60440-900, Fortaleza, CE, Brazil
[d] Departamento de Biologia, Universidade Federal do Ceará, 60440-900, Fortaleza, CE, Brazil
[e] Embrapa Agroindústria Tropical, R. Dra. Sara Mesquita, 2270, 60511-110, Fortaleza, CE, Brazil

ARTICLE INFO

Keywords:
Erythroxylum bezerrae Plowman
Erythroxylaceae
Tropane alkaloids
Cytotoxic activity

ABSTRACT

Six previously undescribed tropane alkaloids, designated as erythrobezerrines A-F, were isolated from the EtOH extract from the stem bark of *Erythroxylum bezerrae* Plowman. Their structures were elucidated based on the interpretation of the NMR and MS data and in some instances, confirmed by X-ray diffraction analysis. The cytotoxicity of the isolated compounds was evaluated against the cancer cell lines L929, PC-3, HCT-116, SNB-19 and NCI-H460, but only erythrobezerrine C showed moderate activity with IC_{50} values of 3.38 and 5.43 μM for HCT-116 and NCI-H460, respectively.

1. Introduction

Erythroxylum, with ca. of 230 species, is the major and most representative genus of the family Erythoxylaceae widespread in the tropical regions of South America, Africa, Southeast Asia, and Madagascar, with main centers of diversity and endemism in Brazil and Venezuela (Loiola et al., 2007; Plowman and Hensold, 2004). To the Brazilian flora, the genus *Erythroxylum* was recently updated, going from 118 (Cordeiro and Loiola, 2018) to 128 species where their main occurrences are in the Amazon rainforest and in the "caatinga", a typical biome of the semi-arid region of the Brazilian Northeast.

Tropane alkaloids (8-methyl-8-azabicyclo[3.2.1]octane) are the active principles of the oldest medicinal plants of the world whose main ethnopharmacological applications include analgesia, hallucinogens, and poisoning. Cocaine, atropine, and scopolamine, compounds of invaluable medical applications, are the more well-known examples of tropane alkaloids (Grynkiewicz and Gadzikowska, 2008). For instance, cocaine is the most popular addictive stimulant drug in the world. Atropine is an anticholinergic drug used for ophthalmologic and heart problems, besides antidote against pesticide poisoning. Scopolamine, which is also an anticholinergic agent, has been used as antiemetic, in addition to presenting off-label indications for gastrointestinal spasms and depression (Kohnen-Johannsen and Kayser, 2019; Lakstygal et al., 2019).

Erythroxylum species are producers of tropane alkaloids which constitute ca. 20% of their specialized metabolites (de Oliveira et al., 2011). These compounds display anti-hypertensive (Oliveira et al., 2012), anticholinergic, anesthetic (Grynkiewicz and Gadzikowska, 2008), and cytotoxic activities (Chavez et al., 2002; Griffin and Lin, 2000; Mi et al., 2002; Sena-Filho et al., 2010).

Motivated by the well-known pharmacological properties, related to the specialized metabolites of the genus, we have investigated *Erythroxylum bezerrae* Plowman, an endemic plant of the northeastern Brazil flora. Herein, the isolation and characterization of six undescribed tropane alkaloid derivatives are reported. Moreover, their antiproliferative properties on a panel of four human cancer cell lines and a murine fibroblast cell line was also evaluated.

2. Results and discussion

The crude EtOH extract from the stem bark of *E. bezerrae* was suspended in MeOH/H_2O (60:40) and partitioned with $CHCl_3$, followed by

* Corresponding author.
E-mail addresses: opessoa@ufc.br, otilialoiola@gmail.com (O.D.L. Pessoa).

https://doi.org/10.1016/j.phytochem.2020.112458
Received 16 January 2020; Received in revised form 8 July 2020; Accepted 12 July 2020
Available online 23 July 2020

EtOAc and, finally, with n-BuOH. TLC analysis, after spraying with the Dragendorff's reagent, indicated the $CHCl_3$ fraction as the one enriched in alkaloids. Chromatographic procedures of this fraction led to the isolation of eight tropane alkaloid derivatives including six previously undescribed (**1**–**6**). The known alkaloids were identified as the 3*α*-(3,4,5-trimethoxycinnamoyloxy)-6*β*-(3,4,5-trimethoxybenzoyloxy)-7*β*-hydroxy-tropane (**7**) and the 3*α*-(3,4,5-trimethoxycinnamoyloxy)-6*β*-(benzoyloxy)-7*β*-hydroxy-tropane (**8**) (Chavez et al., 2002).

The molecular formula $C_{24}H_{27}NO_8$ of compound **1**, colorless crystals, was determined based on the protonated molecule $[M+H]^+$ at *m/z* 458.1815 (calcd 458.1809) by HRESIMS. The ^1H NMR spectrum displayed typical signals of a tropane alkaloid (Table 1): where the signals at δ_H 6.21 (1H, d, $J = 6.0$ Hz, H-6) and 5.53 (1H, t, $J = 4.7$ Hz, H-3) were characteristics of acylated oxymethines, while the signal at 5.32 (1H, d, $J = 6.0$ Hz, H-7) was consistent with a hydroxy methine. In addition, signals for an unsubstituted [δ_H 8.27 (2H, d, $J = 7.2$ Hz, H-2″/H-6″), 7.37 (2H, t, $J = 7.6$ Hz, H-3″″/H5″) and 7.49 (1H, t, $J = 7.4$ Hz, H-4″)], and a symmetrically trisubstituted [δ_H 7.88 (2H, s, H-2'/H-6')] benzoyl ester moieties were clearly evidenced in accordance with a functionalized tropane alkaloid nucleus, typical of those from *Erythroxylum* species (Payo-Hill et al., 2000; Silva et al., 2001; Oliveira et al., 2012).

The ^{13}C NMR spectrum showed nineteen carbon signals which were characterized by DEPT and HSQC spectra as one *N*-methyl (δ_C 38.3), one methoxyl, two methylenes, nine methines, and six non-hydrogenated carbon types (Table 1), where the chemical shifts at δ_C 56.9 (3'/5'-OMe), 108.3 (C-2'/6'), 129.0 (C-3″/5″), 130.4 (C-2″/6″), and 149.3 (C-3'//5') corresponded to two magnetically equivalent carbons each. Based on the HSQC spectrum, the carbon signals at δ_C 80.7 (C-6), 76.4 (C-7), 68.3 (C-3), 68.5 (C-1) and 64.8 (C-5), corresponding to either oxygenated or nitrogenated carbons, exhibited correlations with the proton signals at δ_H 6.21 (1H, d, $J = 6.0$ Hz, H-6), 5.32 (1H, d, $J = 6.0$ Hz, H-7), 5.53 (1H, t, $J = 4.7$ Hz, H-3), 3.41 (1H, s, H-1), and 3.55 (1H, s, H-5), respectively. In the HMBC spectrum, the protons at δ_H 6.21 (H-6) and 5.53 (H-3) exhibited correlations with the carboxyl esters at 166.9 (C-7″), and 166.3 (C-7′), respectively. The position of the two benzoyl substituents at C-3 and C-6, and the hydroxy group at C-7, were assigned based on the multiplicity and coupling constant values displayed by the oxymethine protons. For instance, the protons at δ_H 6.21 (H-6) and 5.32 (H-7), both appearing as doublets, with coupling constants of 6.0 Hz, revealed a vicinal positioning with a *syn*-periplanar relationship [both as *endo* (*α*) oriented]. The triplet showing coupling constant of 4.7 Hz, assigned for H-3 (δ_H 5.53), supports an *α*-positioning for the trisubstituted-benzoyl ester (Chin et al., 2009; Christen et al., 1993; Payo-Hill et al., 2002). The *N*-methyl group at δ_H 2.78 (3H, s) is presented in a *pseudo-equatorial* orientation according to Bringmann et al. (2000). The complete structure of **1**, including its relative stereochemistry, was assigned based on interpretation of its NMR data (Table 1), and single-crystal X-ray diffraction analysis (Fig. 3). Accordingly, the structure of **1** was established as the 3*α*-(4-hydroxy-3,5-dimethoxybenzoyloxy)-6*β*-(benzoyloxy)-7*β*-hydroxy-tropane, named as erythrobezerrine A in allusion to the species *E. bezerrae*.

The molecular formula of compound **2** was determined as $C_{25}H_{29}NO_8$ based on the protonated molecule $[M+H]^+$ at *m/z* 472.1963 (calcd 472.1966) by HRESIMS showing 14 mass units higher (CH_2) than compound **1**. Analyses of the ^1H and ^{13}C NMR data, including the HMBC spectrum, showed a tropane alkaloid with the structure very similar to **1**, but bearing an extra methoxy group in substitution to the hydroxy group of the benzoyl moiety which was supported by the extra methoxy at δ_H 3.98/δ_C 61.0, characteristic of a methoxy group sterically compressed by the two other *ortho* methoxyls. The relative stereochemistry of **2** was stablished by the ROESY spectrum which exhibited dipolar correlations for the *N*-Me protons (3H, s, δ_H 2.78) with both *β*-methylene protons H-2 and H-4 at δ_H 2.36 (2H, m), suggesting a *pseudo-axial* position for the *N*-Me group (Chavez et al., 2002; Ribeiro et al., 2013). The HO-7 and BzO-6 groups were *β*-positioned due to the dipolar correlations for the *α* positioned protons H-6 and H-7 with H-4*α* and H-2*α*, respectively. Thus, the structure of **2** was established as the 3*α*-(3,4,5-trimethoxybenzoyloxy)-6*β*-(benzoyloxy)-7*β*-hydroxy-tropane, designated as erythrobezerrine B (see Fig. 1).

The molecular formula of compound **3**, colorless crystals, was determined as $C_{30}H_{37}NO_{10}$ based on the protonated molecule $[M+H]^+$ at *m/z* 572.2491 (calcd 572.2490). A detailed analysis of the ^1H and ^{13}C NMR spectra showed a tropane alkaloid with a substitution profile similar to **1** and **2**. However, differently of those compounds, its ^1H NMR spectrum exhibited signals for an extra diastereotopic methylene protons at δ_H 2.34 (H-7*β*) and 2.85 (H-7*α*), as well as signals for olefinic protons at δ_H 8.15 (1H, d, H-7′) and 6.97 (1H, d, H-8′) whose coupling constant of 16.0 Hz indicate a double bond with *trans* configuration. In the HMBC spectrum, the olefinic protons (H-7′ and H-8′) exhibited correlations with the ester carbonyl at δ_C 166.3 (C-9′), as well as with the

Table 1
^1H and ^{13}C NMR data assignments for alkaloids **1**, **2**, **4**, and **5** ([a]300 and 75 MHz, [b]500 and 125 MHz), in C_5D_5N.

No.	1[a]		2[b]		4[a]		5[a]	
	δ_C	δ_H	δ_C	δ_H	δ_C	δ_H	δ_C	δ_H
1	68.5	3.41 br s	68.4	3.43 br s	67.1	3.59 br s	66.6	3.60 br s
2*β*	30.8	2.31 m	30.7	2.36 m	34.8	2.30 m	35.0	2.29 m
2*α*		1.87 d (14.0)		1.90 d (14.0)		2.06 d (13.6)		2.08 d (13.9)
3*β*	68.3	5.53 t (4.7)	68.8	5.53 t (4.4)	63.8	4.31 t (4.3)	63.9	4.31 t (4.0)
4*β*	30.7	2.31 m	30.6	2.36 m	34.8	2.30 m	35.0	2.29 m
4*α*		1.91 d (14.0)		1.92 d (14.0)		2.17 d (14.2)		2.17 d (14.0)
5	64.8	3.55 br s	64.7	3.57 br s	66.4	3.63 br s	67.2	3.63 br s
6*α*	80.7	6.21 d (6.0)	80.6	6.15 d (6.0)	79.5	6.85 d (6.3)	79.9	6.86 d (6.0)
7*α*	76.4	5.32 d (6.0)	76.3	5.29 d (6.0)	79.7	6.69 d (6.3)	79.2	6.71 d (6.0)
1′	120.9		126.5		126.2		120.5	
2'/6′	108.3	7.88 s	107.7	7.74 s	107.8	7.58 s	108.4	7.58 s
3'/5′	149.3		154.3		153.9		149.0	
4′	143.3		144.0		143.3		143.3	
7′	166.3		165.9		166.2		166.4	
1"	131.8		131.7		131.1		131.5	
2″/6″	130.4	8.27 d (7.2)	130.4	8.26 d (7.2)	130.4	8.27 d (7.3)	130.4	8.26 d (7.1)
3″/5″	129.0	7.37 t (7.6)	129.0	7.37 t (7.2)	129.2	7.33 t (7.3)	129.2	7.31 t (7.1)
4"	133.3	7.49 t (7.4)	133.4	7.49 t (7.2)	133.7	7.48 t (7.3)	133.6	7.43 t (7.1)
7″	166.9		166.9		166.3		166.7	
4′-MeO			61.0	3.98 s	60.9	3.86 s		
3'/5′-MeO	56.9	4.05 s	56.7	4.00 s	56.1	3.44 s	56.3	3.49 s
3″/5″-MeO								
N-Me	38.3	2.78 s	38.3	2.78 s	39.1	2.78 s	39.3	2.79 s

benzene carbons at δ_C 106.9 (C-2'/6') and 131.0 (C-1'), suggesting a trisubstituted cinnamoyl moiety as depicted in Fig. 2. The molecular structure of **3** (Fig. 4) was assigned from the single-crystal X-ray diffraction analysis (CCDC: 1917800). Unfortunately, the quality of the single crystals was not sufficient to determine the absolute configuration on the basis of the Flack parameter [x = −0.3 (2)], which, even using Cu Kα radiation, was not conclusive (Flack and Bernardinelli, 2008; Geng et al., 2020; Wang et al., 2020). Thus, the structure of **3** was established as the 3α-(3,4,5-trimethoxycinnamoyloxy)-6β-(3,4,5-trimethoxybenzoyloxy)-tropane, named as erythrobezerrine C.

The molecular formula of compound **4** was determined as $C_{25}H_{29}NO_8$ based on the protonated molecule $[M+H]^+$ at *m/z* 472.1961 (calcd 472.1966) in the HRESIMS. The ^1H and ^{13}C NMR spectra of **4** were similar to those of **2**. However, a detailed analysis of the ^1H and ^{13}C NMR data of these two compounds showed remarkable differences in the chemical shifts ($\Delta\delta_C$ 3.4–5.0 ppm) relatively to the oxygenated methine carbons C-3 and C-7, as well as to the methylenes C-2 and C-4 (Table 1) in agreement with the positioning exchange of the hydroxy and the trimethoxy-benzoyl substituents [**2**: δ_C/δ_H 68.8/5.53, t, $J = 4.4$ Hz (C-3) and δ_C/δ_H 76.3/5.29, d, $J = 6.0$ Hz (C-7)]; **4**: $\delta c/\delta_H$ 63.8/4.31, t, $J = 4.3$ Hz (C-3) and δ_C/δ_H 79.7/δ_H 6.69, d, $J = 6.3$ Hz (C-7)]. Thus, differently of compound **2**, both benzoyl moieties were positioned at the vicinal oxymethines C-6 and C-7, in a *syn*-periplanar relationship, as supported by the multiplicity (doublet) and the coupling constant value (6.3 Hz) displayed for the oxymethine protons H-6 and H-7. The relative stereochemistry of **4** was suggested based on the NOESY spectrum which exhibited dipolar correlation of H-7 with H-2α, and H-6 with H-4α, as well as the methyl signal at δ_H 2.78 (Me-N) with both β-positioned H-2 and H-4, indicating the *pseudo-axial* position for the *N*-methyl. Thus, the structure of **4** was established as the 6β-(benzoyloxy)-7β-(3,4,5-trimethoxybenzoyloxy)-3α-hydroxy-tropane, named as erythrobezerrine D.

The HRESIMS of compound **5** displayed a protonated molecule at *m/z* 458.1808 (calcd 458.1809) indicating the molecular formula $C_{24}H_{27}NO_8$. Its ^1H and ^{13}C NMR spectra were similar to **4** (Table 1). The only difference between these compounds was due the substitution of a methoxy group at C-4' (**4**) by a hydroxyl, corroborating with the MS, and as supported by the HMBC correlations of the benzene protons H-2''6' with C-7' (δ_C 166.4) as well as with C-4' (δ_C 143.3). Its relative stereochemistry, depicted in Fig. 2, based on the observed NOE correlations was suggested to be similar to that of compound **4**. Thus, the structure of **5** was established as the 6β-(benzoyloxy)-7β-(4-hydroxy-3,5-dimethoxybenzoyloxy)-3α-hydroxy-tropane, which was named as erythrobezerrine E.

Compound **6**, like compounds **1** and **3,** was also isolated as colorless crystals. Its molecular formula assigned as $C_{29}H_{35}NO_{11}$ was based on the protonated molecule $[M+H]^+$ at *m/z* 574.2262 (calcd 574.2283) in the HRESIMS. The ^1H and ^{13}C NMR spectra of **6** (Table 2) were similar with those of **3** (Table 2). Comparing the ^1H and ^{13}C NMR data of these compounds, the differences were due to the appearance of a signal at δ_H 5.25 (1H, d, $J = 6.0$, H-7) correspondent to an oxymethine proton, and the presence of a hydroxy at C-4" in **6**, replacing the correspondent methoxy group of **3**. The position of the substituents in the tropane core, as well as of each methoxy group in the benzoyl moieties were assigned based on the observed correlations in the HMBC spectrum (Fig. 2). The complete assignments of **6**, including its relative stereochemistry, was

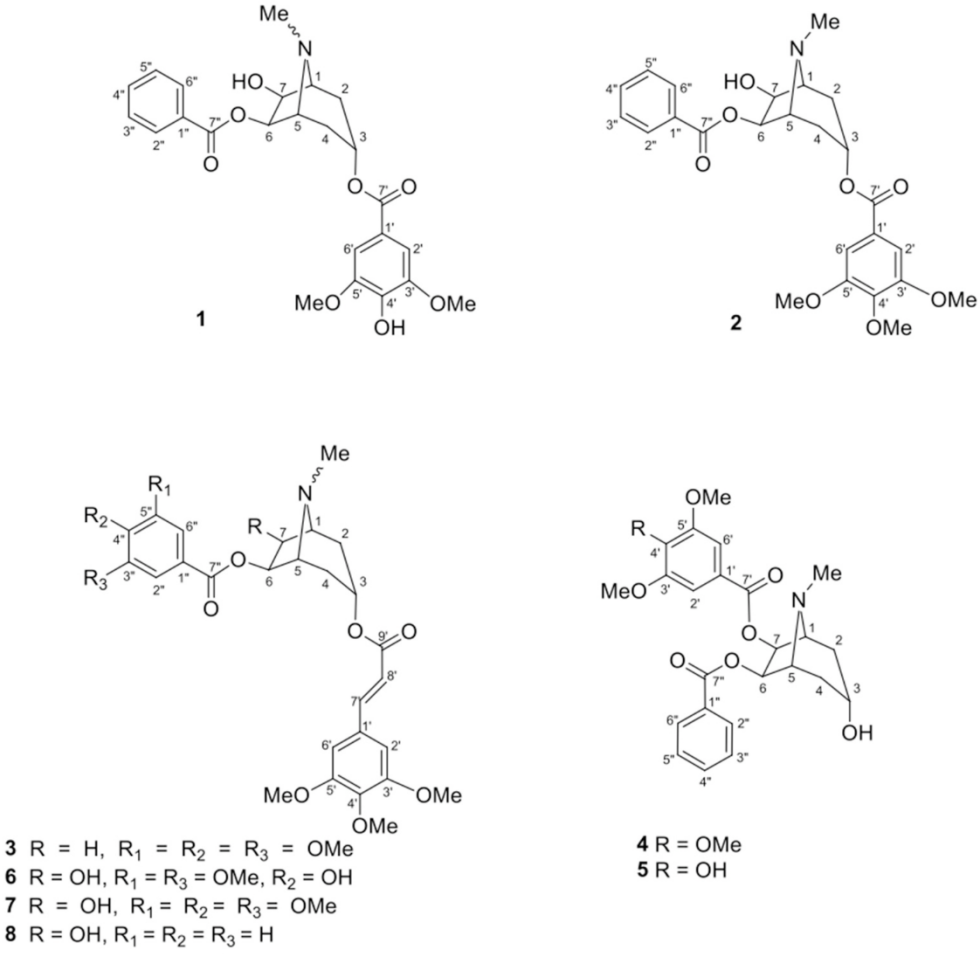

Fig. 1. Structures of the tropane alkaloids (**1**–**8**) isolated from *Erythroxylum bezerrae*.

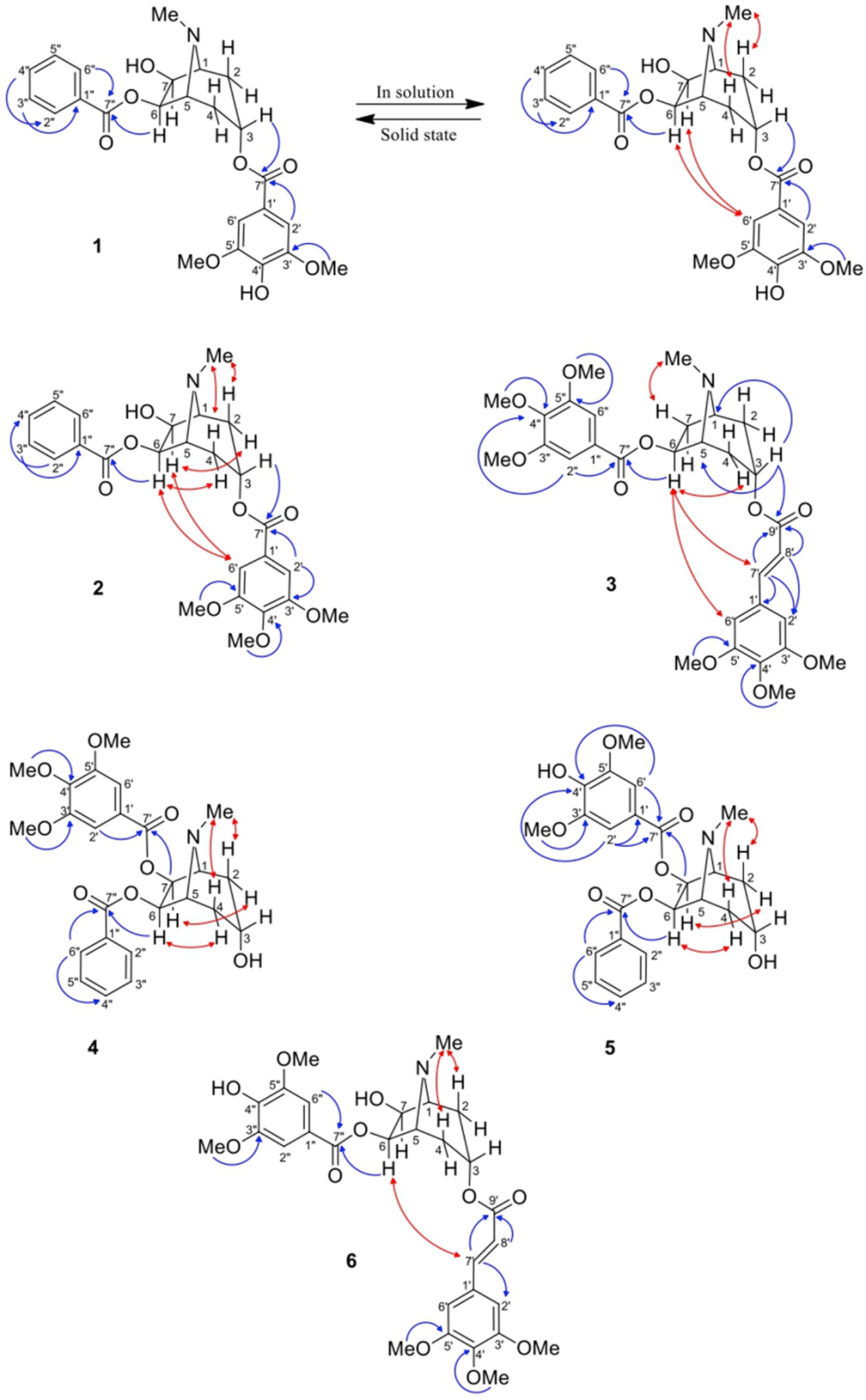

Fig. 2. Important HMBC (↷) and NOESY (↷) correlations of compounds **1–6**.

assigned based on interpretation of its NMR data, and single-crystal X-ray diffraction analysis (Fig. 5). Accordingly, the structure of **6** was established as the 3*α*-(3,4,5-trimethoxycinnamoyloxy)-6*β*-(4-hydroxy-3,5-dimethoxybenzoyloxy)-7*β*-hydroxy-tropane derivative, named as erythrobezerrine F.

In this study were isolated tropane alkaloids bearing a *N*-methyl group in accordance with previous reports on isolated alkaloids of *Erythroxylum* spp. These compounds present a 8-methyl-8-azabicyclo [3.2.1]octane framework, the essential nucleus of several bioactive natural compounds, represented by the well-known atropine, cocaine

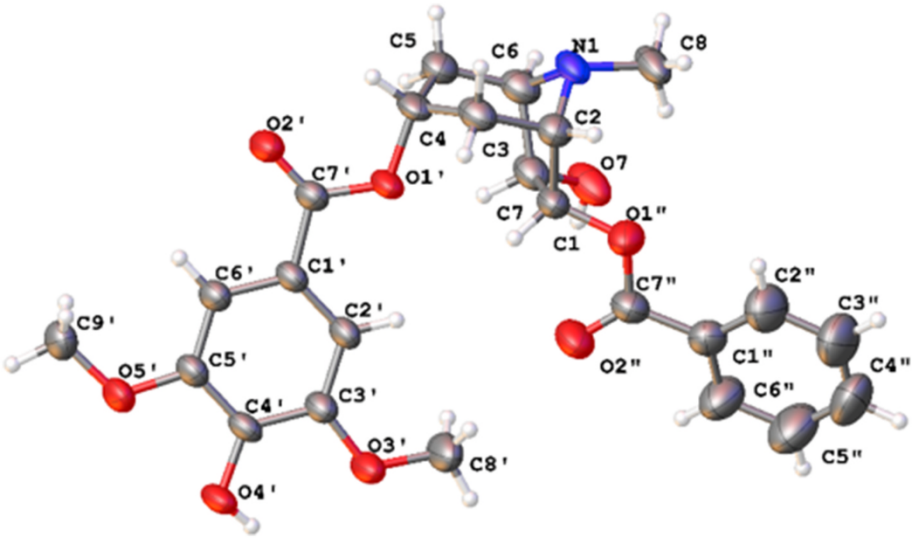

Fig. 3. Asymmetric unit of the crystalline structure of compound **1**.

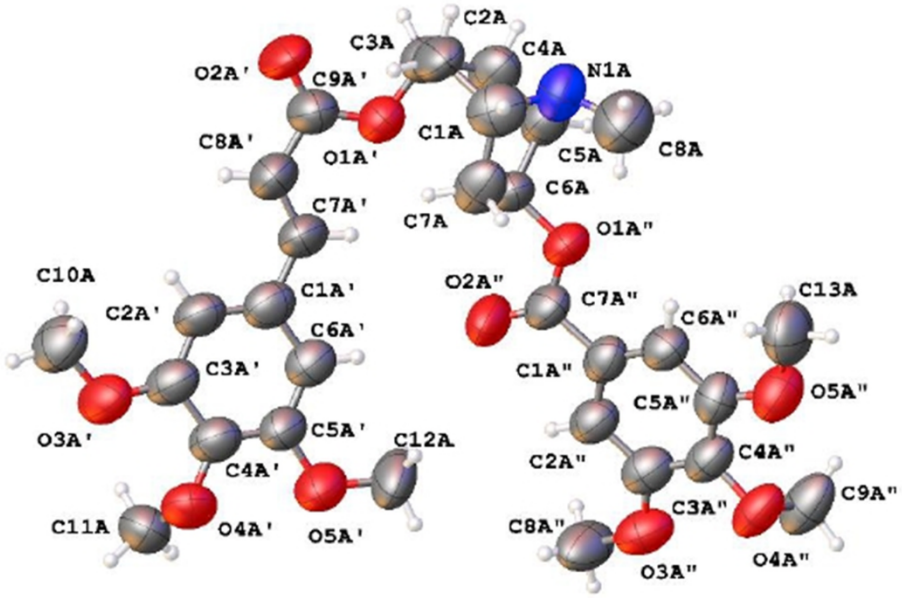

Fig. 4. Asymmetric unit of the crystalline structure only one of the two non-equivalent conformations of **3**.

and scopolamine alkaloids. Tropane-derived compounds, including cocaine analogues have been studied as promising ligands for biological receptors (Zhao et al., 2000; Wee et al., 2006; Grynkiewicz and Gadzikowska, 2008). Thus, the relative stereochemistry of the *N*-alkyl groups of tropane alkaloids have stimulated several studies. For instance, conformational studies by NMR spectroscopy in $CDCl_3$ suggested *pseudo-axial* preferences for the *N*-alkyl groups in tropinone, but preferences for the *pseudo-equatorial* in some C-3 substituted tropanes in a $CFCl_3$ solution (Sidorowicz et al., 2015). In crystal forms, the *N*-methyl conformation was determined to be *pseudo-equatorial* in cocaine (Hrynchuk et al., 1983), but *pseudo-axial* in scopolamine (Glaser et al., 1999).

As discussed above, analysis stereochemistry of **1**, **3** and **6** was indicated based on single-crystal X-ray diffraction and supported by NOESY correlations, while the relative stereochemistry of **2**, **4** and **5** was inferred only by NOESY correlations (Fig. 2). Interestingly, the single-crystal X-ray diffraction of **1** showed the *N*-methyl in the *pseudo-equatorial* position, while its NOESY spectrum exhibited correlations of the *N*-methyl protons with both *β*-positioned H-2 and H-4 indicating a *pseudo*-axial position to that group. Based on these results we can suggest both conformations of the *N*-methyl group for **1**, being the *pseudo-equatorial* conformation preferred in the solid state, while the *pseudo-axial* conformation is preferred in solution, a well-documented phenomenon (Cocinero et al., 2010; Closs, 1959).

For compound **3**, both single-crystal X-ray diffraction and NOESY spectrum converged to the *N*-methyl in the pseudo-equatorial position whereas compound **6** to the *pseudo-axial*. The *pseudo-axial* conformation for the *N*-methyl in compounds **2**, **4** and **5** was established based on NOESY correlations.

Interestingly, compounds **1**, **4**–**6** displayed small values of optical rotation (−4.3° to −9.7°) suggesting scalemic mixtures. To clarify this point, compounds **1** and **6** were analyzed by HPLC using a chiral column, however, both **1** and **6** exhibit a single peak in their chromatograms. Thus, the results seem to be inconclusive to state that compounds **1**, **4**–**6**

Table 2
^{1}H and ^{13}C NMR data assignments for alkaloids **3** and **6** (300 and 75 MHz), in C_5D_5N.

No.	3		6	
	δ_C	δ_H	δ_C	δ_H
1	60.4	3.33 br s	68.2	3.36 br s
2β	34.1	2.26 m	29.9	2.28 dt (14.4; 4.2)
2α		1.75 d (15.0)		1.82 d (15.4)
3β	67.8	5.37 t (4.3)	68.5	5.41 t (4.2)
4β	32.9	2.33 m	29.5	2.28 dt (14.4; 4.2)
4α		2.02 d (15.5)		1.82 d (15.4)
5	66.0	3.50 br s	64.3	3.59 br s
6	80.9	6.06 dd (7.8; 2.7)	80.3	6.26 d (6.0)
7 α	37.5	2.85 dd (14.2; 7.8)	76.4	5.25 d (6.0)
7 β		2.34 m		
1′	131.0		131.1	
2′/6′	106.9	7.23 s	107.1	7.44 s
3′/5′	154.6		154.6	
4′	141.4		141.4	
7′	145.9	8.15 d (16.0)	146.0	8.29 d (15.0)
8′	118.8	6.97 d (16.0)	118.8	6.87 d (15.0)
9′	166.3		166.0	
1″	126.5		121.2	
2″/6″	107.8	7.54 s	108.6	7.71 s
3″/5″	154.1		149.1	
4″	143.5		143.1	
7″	166.6		167.4	
4′-MeO	61.0	3.95 s	61.1	3.99 s
3′/5′-MeO	56.5	3.89 s	56.6	3.97 s
4″-MeO	61.0	3.95 s		
3″/5″-MeO	56.5	3.80 s	56.5	3.74 s
Me-N	39.6	2.61 s	37.6	2.71 s

were isolated as scalemic mixture.

In addition to the undescribed compounds, the known tropane alkaloids 3α-(3,4,5-trimethoxycinnamoyloxy)-6β-(3,4,5-trimethoxybenzoyloxy)-7β-hydroxy-tropane (**7**) and the 3α-(3,4,5-trimethoxycinnamoyloxy)-6β-(benzoyloxy)-7β-hydroxy-tropane (**8**) (Chavez et al., 2002) were also isolated.

The antiproliferative properties of the isolated alkaloids were evaluated against four human cancer cell lines [human metastatic prostate cancer (PC-3), colon adenocarcinoma (HCT-116), human glioblastoma (SNB-19) and human lung cancer (NCI-H460)] and a murine fibroblast cell line (L929). As can be seen from Table 3, only erythrobezerrine C (**3**) displayed moderate cytotoxicity against HCT-116 (IC_{50} 3.38 μM) and NCI-H460 (IC_{50} 5.43 μM) cancer cell lines.

3. Conclusions

Phytochemical analysis of the EtOH extract from the stem bark of *E. bezerrae* revealed six tropane alkaloids derivatives (**1**–**6**) still undescribed in the literature, along with two known ones (**7** and **8**). Tropane alkaloids bearing hydroxyl groups or benzoyl esters derivatives are a characteristic of *Erythroxylum* plants. Many of these compounds display cytotoxic activity, however their most relevant activities are anesthetic, anticholinergic, antihypertensive. Trying to find anticancer natural products, we have tested the isolated alkaloids of *E. bezerrae* on cancer cell lines. In relation to potential anti-cancer actions, the low toxicity of the tropane alkaloids 1–6, notably towards a murine fibroblast cell line, merits further investigation.

4. Experimental section

4.1. General experimental procedures

Optical rotations were measured using a JASCO P-2000 digital polarimeter. Melting points were recorded on a digital Microquimica MQAPF-302 apparatus and were uncorrected. IR spectra were recorded using a PerkinElmer Spectrum 100 FTIR spectrometer equipped with universal attenuated total reflectance accessory (UATR) in the range from 4000 to 600 cm-1. UV spectra were obtained with a Shimadzu UV-2600 spectrometer. NMR spectra, in pyridine-d_5, were run at room temperature either on a Bruker Avance DRX-500 or Avance DPX-300 spectrometers, and the data were processed using a Bruker Top Spin software. HRMS were acquired using on an Acquity Xevo UPLC-QTOF-MS system from Waters. HPLC analyses were carried out using a UFLC

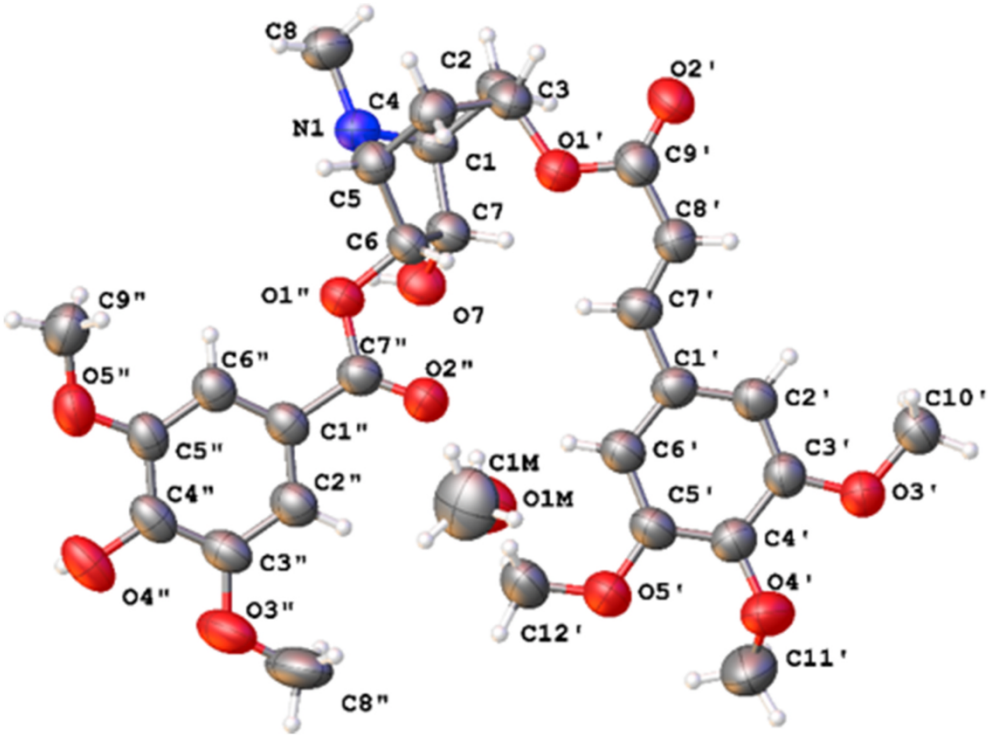

Fig. 5. Asymmetric unit of the crystalline structure of compound **6**.

Table 3
Cytotoxic activity (IC_{50} μM) of the isolated tropane alkaloids (**1**–**8**) against selected tumor cell lines evaluated by the MTT assay after 72 h exposure.

Compounds	L929	PC-3	HCT-116	SNB-19	NCI-H460
1	>40	17.14 (15.11–19.46)	28.95 (26.21–31.97)	36.67 (21.81–61.66)	15.45 (12.60–18.93)
2	>40	>40	28.07 (25.58–30.81)	21.23 (17.60–25.63)	21.95 (18.80–25.63)
3	20.71 (18.42–23.31)	15.02 (13.36–16.89)	3.38 (3.05–4.20)	10.47 (9.64–11.37)	5.43 (4.88–6.04)
4	>40	>40	>40	>40	>40
5	>40	>40	38.88 (36.50–41.42)	>40	>40
6	>40	>40	17.75 (15.52–20.31)	28.41 (25.38–31.80)	29.81 (26.30–33.79)
7	19.40 (14.69–25.89)	10.56 (9.75–11.45)	16.45 (14.15–17.87)	13.89 (12.65–15.26)	10.55 (9.43–11.80)
8	30.58 (25.29–30.80)	>40	19.26 (17.75–20.91)	31.37 (25.92–31.99)	17.33 (15.74–19.08)
Dox	1.72 (1.58–1.87)	0.76 (0.59–0.93)	0.21 (0.16–0.29)	0.15 (0.13–0.18)	2.06 (1.73–2.45)

Dox = Doxorubicin.

(SHIMADZU) system equipped with an SPD-M20A diode array UV–Vis detector, a Phenomenex C18 column, 5 μm (250 × 10 mm) to purification of compounds, and a CHIRALCEL OD-H chiral-phase column, 5 μm (150 × 4.6 mm) to chiral purity analysis. Open column chromatography were carried out with silica gel 60 (70–230 mesh, Merck) and SPE cartridges C18 (10 g/60 mL; Strata, Phenomenex), while TLC were conducted on precoated silica gel aluminum sheets ($60F_{254}$, 0.20 mm, Merck).

4.2. Plant material

The stem bark of *Erythroxylum bezerrae* Plowman (Erythroxylaceae) was collected from Serra das Almas (S 5°8′28.60″ and W 40°54′57.20″) in the Ibiapaba plateau, Ceará State – Brazil, on April, 2017 (raining season). The plant was identified by the co-author Dr. M. I. B. Loiola of the Laboratório de Sistemática e Ecologia Vegetal Departmento de Biologia - Universidade Federal do Ceará. A voucher specimen No. EAC 58211 (SIGEN: A50E3D9) has been deposited at the Prisco Bezerra Herbarium, Universidade Federal do Ceará.

4.3. Extraction and isolation

The air-dried and powdered stem bark (1.8 Kg) of *E. bezerrae* was extracted by maceration with EtOH (2 x 8L). The solvent was distillated under reduced pressure to afford 46.5 g of a crude extract that was suspended in a mixture of MeOH/H_2O 60:40 (200 mL), then partitioned with $CHCl_3$, EtOAc (100 mL x 3 for each solvent) and n-BuOH (50 mL) to afford, after the solvents evaporation, 18.3, 2.6 and 2.4 g of the extract fractions, respectively. TLC comparison of all fractions, after spraying with the Dragendorff's reagent, revealed the presence of alkaloids in the $CHCl_3$ fraction. An aliquot of this fraction (10.0 g) was chromatographed on a silica gel column (22.0 g) eluted with binary mixtures of CH_2Cl_2/MeOH (95:5, 90:10, 80:20, 50:50) and MeOH. Fraction CH_2Cl_2/MeOH 90:10 (4.0 g) was further re-chromatographed using the same eluents as before, to afford four subfractions (95:5, 90:10, 80:20, 50:50).

The fraction CH_2Cl_2/MeOH 90:10 (1.9 g) showed to be rich in alkaloids after TLC spraying with Dragendorff's reagent. This fraction was subjected to a silica gel flash column, eluted with CH_2Cl_2/i-PrOH, to yield two main fractions: FA (612.0 mg) and FB (314.0 mg). An aliquot of FA (200 mg) was subjected to HPLC analysis using a semi-preparative C-18 column, solvent system of H_2O (0.05% TEA)/ACN 50–100%, flow rate of 3.0 mL/min at 210–400 nm to afford compounds **1** (13.0 mg, $t_R = 6.9$ min), **2** (7.0 mg, $t_R = 9.4$ min), **3** (8.3 mg, $t_R = 13.4$ min), **7** (7.8 mg, $t_R = 10.6$ min) and **8** (6.7 mg, $t_R = 11.2$ min). Compound **4** (5.0 mg, $t_R = 13.0$ min) was isolated from an aliquot of FB (100 mg) using the same procedure. Fraction CH_2Cl_2/MeOH 80:20 (2.4 g), from the first chromatographic fractionation, was subjected to a C-18 SPE cartridge by elution with H_2O/MeOH (50:50, 40:60, 30:70, 20:80, 10:90), and MeOH. An aliquot (100 mg) of fraction H_2O/MeOH (50:50) was subjected to HPLC using a semi-preparative C-18 column, a gradient solvent system of H_2O (0.05% TEA)/ACN 20–100%, flow rate 3.0 mL/min at 210–400 nm to afford compound **5** (11.0 mg, tR = 14.0 min), further amount, of compound **1** (8.5 mg, $t_R = 15.5$ min), and compound **6** (7.8 mg, $t_R = 17.2$ min).

4.4. Isolated compounds

4.4.1. Erythrobezerrine A (1)

Colorless crystals; mp 226–228 °C; $[\alpha]_D^{22}$ -8.8° (*c* 0.06, $CHCl_3$/MeOH 1:1); UV ($CHCl_3$) λ_{max} (log ε) 280 (1.04), 239 (1.13); IR (KBr) ν_{max} 3563, 3410, 2928, 1710, 1460, 1248, 1128, 758 cm^{-1}; HRESIMS *m/z* 458.1815 $[M+H]^+$ (calcd for $C_{24}H_{28}NO_8$, 458.1809); ^1H and ^{13}C NMR spectroscopic data, see Table 1.

4.4.2. Erythrobezerrine B (2)

Yellow resin; $[\alpha]_D^{21}$ +39.8° (*c* 0.14, $CHCl_3$/MeOH 1:1); UV ($CHCl_3$) λ_{max} (log ε) 280 (1.02), 239 (1.22); IR (KBr) ν_{max} 3487, 2938, 1706, 1675, 1462, 1210, 1125, 783, 720 cm^{-1}; HRESIMS *m/z* 472.1963 $[M+H]^+$ (calcd for $C_{25}H_{30}NO_8$, 472.1966); ^1H and ^{13}C NMR spectroscopic data, see Table 1.

4.4.3. Erythrobezerrine C (3)

Colorless crystals; mp 140–142 °C; $[\alpha]_D^{22}$ +23.6° (*c* 0.1, $CHCl_3$/MeOH 1:1); UV ($CHCl_3$) λ_{max} (log ε) 306 (1.46), 276 (1.37), 239 (1.50); IR (KBr) ν_{max} 3496, 2934, 1716, 1460, 1220, 1128, 768, 710 cm^{-1}; HRESIMS *m/z* 572.2491 $[M+H]^+$ (calcd for $C_{30}H_{38}NO_{10}$, 572.2490); ^1H and ^{13}C NMR spectroscopic data, see Table 2.

4.4.4. Erythrobezerrine D (4)

Yellow resin; $[\alpha]_D^{20}$ -9.7° (*c* 0.1, $CHCl_3$/MeOH 1:1); UV ($CHCl_3$) λ_{max} (log ε) 302 (0.63), 272 (1.05), 239 (1.15); IR (KBr) ν_{max} 3410, 2928, 1710, 1460, 1128, 758 cm^{-1}; HRESIMS *m/z* 472.1961 $[M+H]^+$ (calcd for $C_{25}H_{30}NO_8$, 472.1966); ^1H and ^{13}C NMR spectroscopic data, see Table 1.

4.4.5. Erythrobezerrine E (5)

Yellow resin; $[\alpha]_D^{20}$ -7.0° (*c* 0.1, $CHCl_3$/MeOH 1:1); UV ($CHCl_3$) λ_{max} (log ε) 333 (0.21), 275 (0.98), 238 (1.11); IR (KBr) ν_{max} 3431, 2939, 1714, 1464, 1221, 1117, 764, 713 cm^{-1}; HRESIMS *m/z* 458.1808 $[M+H]^+$ (calcd for $C_{24}H_{28}NO_8$, 458.1809); ^1H and ^{13}C NMR spectroscopic data, see Table 1.

4.4.6. Erythrobezerrine F (6)

Colorless crystals; mp 199–201 °C; $[\alpha]_D^{22}$ -4.3°, (*c* 0.1, $CHCl_3$/MeOH 1:1); UV ($CHCl_3$) λ_{max} (log ε) 326 (0.53), 300 (0.68), 279 (0.74), 238 (1.11); IR (KBr) ν_{max} 3485, 2937, 1710, 1670, 1461, 1123, 777, 721 cm^{-1}; HRESIMS *m/z* 574.2262 $[M+H]^+$ (calcd for $C_{29}H_{36}NO_{11}$, 574.2283); ^1H and ^{13}C NMR spectroscopic data, see Table 2.

4.5. Chiral analysis of compounds 1 and 6

Compounds **1** and **6** were subjected to HPLC analysis using a chiral OD-H column eluting with an isocratic solvent system: *n*-hexane (100% in 30 min, flow rate 0.5 mL/min) and isopropanol/*n*-hexane (0.5:99.5) in 30 min, flow rate 0.5 mL/min.

4.6. X-ray crystallography of compounds 1, 3 and 6

The single-crystal X-ray intensity data of compounds **1**, **3** and **6** were measured on a Bruker D8 Venture equipped with a microfocus Mo generator (λKα = 0.71073 Å) or a microfocus Cu generator (λKα = 1.54178 Å) and a Photon II CMOS detector. Data collection on compound **1** was performed with Mo radiation, whereas data collection on compounds **3** and **6** was performed with Cu radiation. The frames were integrated with the Bruker SAINT software package (Bruker, V8.38A, after 2013) using a narrow-frame algorithm. The final cell parameters for each crystal were based upon the refinement of the XYZ-centroids of some reflections. Data were corrected for absorption effects using the Multi-Scan method. The structure was solved by intrinsic phasing using SHELXT (Sheldrick, 2015) and refined with the ShelXL (Sheldrick, 2008) refinement package using Least Squares minimization by using Olex2 (Dolomanov et al., 2009) as a graphical interface. All non-hydrogen atoms were refined anisotropically. Hydrogen atom positions were calculated geometrically and refined using the riding model. The programs ORTEP-III (Farrugia, 1997) and Olex2 (Dolomanov et al., 2009) were used to prepare the artwork representations for publication. Crystallographic data of **1**, **3** and **6** have been deposited at the Cambridge Crystallographic Data Center (For **1**, CCDC Number: 1917799; for **3**, CCDC Number: 1917800 and for **6**, CCDC Number: 1917801). Copies of the data can be obtained, free of charge, through application to the Director, CCDC, 12 Union Road, Cambridge CB2 1EZ, UK, (fax: +44-(0) 1223–336033, or e-mail: deposit@ccdc.cam.ac.uk or http://www.ccdc.cam.ac.uk).

4.6.1. Crystallographic data of 1

Colourless prism crystals of compound **1** were obtained from a $CHCl_3$/MeOH (6:4) solution after slow evaporation in a refrigerator for 2 weeks. $C_{24}H_{27}NO_8$, $M_r = 457.47\ g\ mol^{-1}$; size 0.386 × 0.185 × 0.164 mm; monoclinic, space group *C2/c*, $a = 27.743(3)$ Å, $b = 11.3371(13)$ Å, $c = 13.9706(16)$ Å, $\alpha = 90°$, $\beta = 90.836(4)°$, $\gamma = 90°$; $V = 4393.7(8)$ $Å^3$, $Z = 8$, $\rho_{calc} = 1.410\ g\ cm^{-3}$, μ (Mo Kα) = 0.104 mm^{-1}, multi-scan, *trans* $_{min} = 0.618$, *trans* $_{max} = 0.746$, $F(000) = 1936.0$. The total number of reflections was 32389 ($-36 \le h \le 36$, $-14 \le k \le 14$, $-17 \le l \le 18$) measured in the range $5.686° \le \Theta \le 54.97°$, completeness $\Theta_{max} = 99.4\%$, 5020 unique ($R_{int} = 0.0793$, $R_{sigma} = 0.0586$) which were used in all calculations; Final indices: $R_{1obs} = 0.0794$, $wR_{2obs} = 0.2253$ [$I \ge 2\sigma(I)$]; $R_{1all} = 0.1231$, $wR_{2all} = 0.2586$ [all data], GOOF = 1.082, largest difference peak and hole 0.45/-0.26 e $Å^{-3}$.

4.6.2. Crystallographic data of 3

Colourless prism crystals of compound **3** were obtained from a $CHCl_3$/MeOH (6:4) solution after slow evaporation in a refrigerator for 2 weeks. $C_{30}H_{37}NO_{10}$, $M_r = 571.60\ g\ mol^{-1}$; size 0.428 × 0.073 × 0.067 mm; triclinic, space group *P1*, $a = 7.4488(8)$ Å, $b = 12.8356(13)$ Å, $c = 16.5521(19)$ Å, $\alpha = 86.459(8)°$, $\beta = 80.381(7)°$, $\gamma = 77.294(7)°$; $V = 2251.67(14)$ $Å^3$, $Z = 2$, $\rho_{calc} = 1.248\ g\ cm^{-3}$, μ (Cu Kα) = 0.780 mm^{-1}, multi-scan, $trans_{min} = 0.774$, $trans_{max} = 1.000$, $F(000) = 608.0$. The total number of reflections was 22687 ($-9 \le h \le 9$, $-15 \le k \le 14$, $-20 \le l \le 20$) measured in the range $3.531° \le \Theta \le 72.788°$, completeness $\Theta_{max} = 99.2\%$, 10524 unique ($R_{int} = 0.0551$, $R_{sigma} = 0.0857$) which were used in all calculations; Final indices: $R_{1obs} = 0.0765$, $wR_{2obs} = 0.2002$ [$I \ge 2\sigma(I)$]; $R_{1all} = 0.1690$, $wR_{2all} = 0.2742$ [all data], GOOF = 0.944, Flack parameter = −0.3(2), largest difference peak and hole 0.50/-0.16 e $Å^{-3}$.

4.6.3. Crystallographic data of 6

Colourless prism crystals of compound **6** were obtained from a $CHCl_3$/MeOH (6:4) solution after slow evaporation in a refrigerator for 2 weeks. Under this condition, compound **6** crystallized as a methanol solvate. $C_{29}H_{35}NO_{11} \cdot CH_4O$, $M_r = 605.62\ g\ mol^{-1}$; size 0.204 × 0.145 × 0.06 mm; triclinic, space group $P\overline{1}$, $a = 10.5925(12)$ Å, $b = 11.6922(14)$ Å, $c = 13.4914(17)$ Å, $\alpha = 68.682(7)°$, $\beta = 68.225(7)°$, $\gamma = 80.518(6)°$; $V = 1444.6(3)$ $Å^3$, $Z = 2$, $\rho_{calc} = 1.392\ g\ cm^{-3}$, μ (Cu Kα) = 0.906 mm^{-1}, multi-scan, *trans* $_{min} = 0.846$, *trans* $_{max} = 0.947$, $F(000) = 644.0$. The total number of reflections was 28459 ($-13 \le h \le 13$, $-13 \le k \le 14$, $-17 \le l \le 17$) measured in the range $3.8737° \le \Theta \le 79.764°$, completeness $\Theta_{max} = 94.2\%$, 5939 unique ($R_{int} = 0.0680$, $R_{sigma} = 0.0487$) which were used in all calculations; Final indices: $R_{1obs} = 0.0965$, $wR_{2obs} = 0.2426$ [$I \ge 2\sigma(I)$]; $R_{1all} = 0.1587$, $wR_{2all} = 0.2950$ [all data], GOOF = 1.088, largest difference peak and hole 0.32/-0.45 e $Å^{-3}$.

4.7. Bioassay

4.7.1. Cytotoxic assay

The cytotoxicity activity was evaluated against four different human cancer cell lines provided by the National Cancer Institute U.S. (Bethesda, MD): metastatic prostate cancer (PC-3), colon adenocarcinoma (HCT-116), glioblastoma (SNB-19) and lung cancer (NCI-H460), and a murine fibroblast cell line (L929). Cells were maintained in RPMI 1640 (L929-were grown in DMEM) medium supplemented with 10% fetal bovine serum (v/v), 2 mM glutamine, 100 U/mL penicillin and 100 μg/mL streptomycin at 37 °C under a 5% CO_2 atmosphere. Compounds (**1**–**8**) were tested at concentrations ranging from 0.02 to 10 μM during 72 h and the effect on cell proliferation was evaluated *in vitro* using the MTT [3-(4,5-dimethyl-2-thiazolyl)-2,5-diphenyl-*2H*-tetrazolium bromide] assay, as described by Mosmann (1983). Doxorubicin, a standard compound with a well-established anticancer activity was used as positive control. IC_{50} (the concentration that inhibits growth in 50%) was calculated, along with the respective 95% CI (confidence interval), by non-linear regression using the software GraphPad Prism 5.0.

Declaration of competing interest

The authors declare that they have no known competing financial interests or personal relationships that could have appeared to influence the work reported in this paper.

Acknowledgements

This study was supported by grants from Coordenação de Aperfeiçoamento de Pessoal de Nível Superior/Fundação Cearense de Apoio ao Desenvolvimento Científico e Tecnológico - CAPES/FUNCAP (No. 88887.113263/2015–01) and Conselho Nacional de Desenvolvimento Científico e Tecnológico – CNPq (No. 420454/2016-0 and 309060/2016-8).

Appendix A. Supplementary data

Supplementary data to this article can be found online at https://doi.org/10.1016/j.phytochem.2020.112458.

References

Bringmann, G., Gunther, C., Muhlbacher, J., Gunathilake, M.D.L.P., Wickramasinghe, A., 2000. Tropane alkaloids from *Erythroxylum zeylanicum* O. E. Schulz (Erythroxylaceae). Phytochemistry 53, 409–416. https://doi.org/10.1016/S0031-9422(99)00561-0.

Chávez, D., Cui, B., Chai, H.-B., García, R., Mejía, M., Farnsworth, N.R., Cordell, G.A., Pezzuto, J.M., Kinghorn, A.D., 2002. Reversal of multidrug resistance by tropane alkaloids from the stems of *Erythroxylum rotundifolium*. J. Nat. Prod. 65, 606–610. https://doi.org/10.1021/np0104774.

Chin, Y., Jones, W.P., Waybright, T.J., Mccloud, T.G., Cragg, G.M., Cassady, J.M., Kinghorn, A.D., 2009. Tropane aromatic ester alkaloids obtained from a large-scale recollection of *Erythroxylum pervillei* stem bark collected in Madagascar. J. Nat. Prod. 69, 414–417. https://doi.org/10.1021/np050366v.

Christen, P., Roberts, M.F., Phillipson, J.D., Evans, W.C., 1993. Alkaloids of *Erythroxylum zambesiacum* stem-bark. Phytochemistry 34, 1147–1151. https://doi.org/10.1016/S0031-9422(00)90733-7.

Closs, G.L., 1959. The configurational equilibrium of the N-methyl group in some tropane Deuteriohalides[1]. J. Am. Chem. Soc. 20, 5456–5461. https://doi.org/10.1021/ja01529a052.

Cocinero, E.J., Lesarri, A., Écija, P., Grabow, J.U., Fernández, J.A., Castaño, F., 2010. N-Methyl stereochemistry in tropinone: the conformational flexibility of the tropane motif. Phys. Chem. Chem. Phys. 12, 6076–6083. https://doi.org/10.1039/C000528B.

Cordeiro, L.S., Loiola, M.I.B., 2018. Flora do Ceará, brasil: Erythroxylaceae. Rodriguesia 69, 881–903. https://doi.org/10.1590/2175-7860201869242.

Dolomanov, O.V., Bourhis, L.J., Gildea, R.J., Howard, J.A.K., Puschmann, H., 2009. Olex2: a complete structure solution, refinement and analysis program. J. Appl. Crystallogr. 42, 339–341. https://doi.org/10.1107/S0021889808042726.

de Oliveira, S.L., Tavares, J.F., Branco, M.V.S.C., Lucena, H.F.S., Barbosa-Filho, J.M., Agra, M. de F., do Nascimento, S.C., dos S, Aguiar J., da Silva, T.G., de Simone, C.A., de Araújo-Júnior, J.X., da Silva, M.S., 2011. Tropane alkaloids from *Erythroxylum caatingae* plowman. Chem. Biodivers. 8, 155–165. https://doi.org/10.1002/cbdv.200900400.

Farrugia, L.J., 1997. Ortep-3 for windows - aversion of Ortep - III with a graphical user interface (GUI). J. Appl. Cryst. 30, 565. https://doi.org/10.1107/S0021889897003117.

Flack, H.D., Bernardinelli, G., 2008. The use of X-ray crystallography to determine absolute configuration. Chirality 20, 681–690. https://doi.org/10.1002/chir.20473.

Geng, H., Liu, Y.C., Li, D.S., Xiao, C.J., Liu, Y., Li, X.N., Li, S.H., 2020. Unusual glycosidic labdane diterpenoids with cytotoxicity from the root of Phlomoides betonicoides. Phytochemistry 173, 112325. https://doi.org/10.1016/j.phytochem.2020.112325.

Glaser, R., Shiftan, D., Drouin, M., 1999. Conformational pseudopolymorphism and solid-state CPMAS NMR studies for determination of solvent-dependent solution-state conformational preferences for (−)-scopolamine hydrobromide/hydrochloride salts. Org. Chem. 64, 9217–9224. https://doi.org/10.1021/jo9912956.

Griffin, W.J., Lin, G.D., 2000. Chemotaxonomy and geographical distribution of tropane alkaloids. Phytochemistry 53, 623–637. https://doi.org/10.1016/S0031-9422(99)00475-6.

Grynkiewicz, G., Gadzikowska, M., 2008. Tropane alkaloids as medicinally useful natural products and their synthetic derivatives as new drugs. Pharmacol. Rep. 60, 439–463. https://doi.org/10.1002/chin.200940262.

Hrynchuk, R.J., Barton, R.J., Robertson, B.E., 1983. The crystal structure of free base cocaine, $C_{17}H_{21}NO_4$. Can. J. Chem. 61, 481–487. https://doi.org/10.1139/v83-085.

Kohnen-Johannsen, K.L., Kayser, O., 2019. Tropane alkaloids: chemistry, pharmacology, biosynthesis and production. Molecules 24, 796. https://doi.org/10.3390/molecules24040796.

Lakstygal, A.M., Kolesnikova, T.O., Khatsko, S.L., Zabegalov, K.N., Volgin, A.D., Demin, K.A., Shevyrin, V.A., Wappler-Guzzetta, E.A., Kalueff, A.V., 2019. Dark classics in chemical neuroscience: atropine, scopolamine, and other anticholinergic deliriant hallucinogens. ACS Chem. Neurosci. 10, 2144–2159. https://doi.org/10.1021/acschemneuro.8b00615.

Loiola, M.I.B., Agra, M. de F., Baracho, G.S., Queiroz, R.T. de, 2007. Flora da Paraíba, Brasil: erythroxylaceae Kunth. Acta Bot. Bras. 21, 473–487. https://doi.org/10.1590/s0102-33062007000200020.

Mi, Q., Cui, B., Silva, G.L., Lantvit, D., Lim, E., Chai, H., Hollingshead, M.G., Mayo, J.G., Kinghorn, A.D., Pezzuto, J.M., 2002. Pervilleines B and C, new tropane alkaloid aromatic esters that reverse the multidrug-resistance in the hollow fiber assay. Canc. Lett. 184, 13–20. https://doi.org/10.1016/S0304-3835(02)00202-1.

Mosmann, T., 1983. Rapid colorimetric assay for cellular growth and survival: Application to proliferation and cytotoxicity assays. J. Immunol. Methods 65, 55–63. https://doi.org/10.1016/0022-1759(83)90303-4.

Oliveira, A.C., Sena-Filho, J.G., Mendes-Júnior, L.G., Anjos, R.M., Ribeiro, T.P., Barbosa-Filho, J.M., Braga, V.A., Medeiros, I.A., 2012. *Erythroxylum pungens* elicits vasorelaxation by reducing intracellular calcium concentration in vascular smooth muscle cells of rats. Braz. J. Pharmacog. 22, 436–442. https://doi.org/10.1590/S0102- 695X2012005000005.

Payo-Hill, A.L., Dominguez, R.S., Suarez, M.O., Batista-Baez, M., Castro, H.T.V., Rastrelli, L., Aquino, R., 2002. Tropane alkaloids from the leaves and stem bark of *Erythroxylon alaternifolium* and *Erythroxylon rotundifolium*. Phytochemistry 54, 927–932. https://doi.org/10.1016/s0031-9422(00)00087-x.

Plowman, T., Hensold, N., 2004. Names, types, and distribution of neotropical species of *Erythroxylum* (Erythroxylaceae). Brittonia 56, 1–53. https://doi.org/10.1663/0007-196x(2004)056[0001:ntadon]2.0.co;2.

Ribeiro, E.M. de O., Lima, L.S., David, J.M., Vale, A.E. do, Lopes, L.M.X., David, J.P., 2013. A new tropane alkaloid and other constituents of *Erythroxylum rimosum* (Erythroxylaceae). Phytochem. Lett. 6, 232–235. https://doi.org/10.1016/j.phytol.2013.02.008.

Sena-Filho, J.G., Da Silva, M.S., Tavares, J.F., Oliveira, S.L., Romero, M.A.V., Xavier, H. S., Barbosa-Filho, J.M., Braz-Filho, R., 2010. Cytotoxic evaluation of pungencine: a new tropane alkaloid from the roots of *Erythroxylum pungens*. O. E. Schulz. Helv. Chim. Acta 93, 1742–1744. https://doi.org/10.1002/hlca.200900434.

Sidorowicz, K., Ratkiewicz, A., Nodzewska, A., Lazny, R., 2015. Determination of the N-invertomer stereochemistry in N-substituted nortropanones and norgranatanones using computational and NMR methods. C. R. Chim. 18, 693–704. https://doi.org/10.1016/j.crci.2014.10.006.

Silva, G.L., Cui, B., Chávez, D., You, M., Chai, H.B., Rasoanaivo, P., Lynn, S.M., O'Neill, M.J., Lewis, J.A., Besterman, J.M., Monks, A., Farnsworth, N.R., Cordell, G. A., Pezzuto, J.M., Kinghorn, A.D., 2001. Modulation of the multidrug-resistance phenotype by new tropane alkaloid aromatic esters from *Erythroxylum pervillei*. J. Nat. Prod. 64, 1514–1520. https://doi.org/10.1021/np010295+.

Sheldrick, G.M., 2008. A short history of ShelX. Acta Crystallogr. A64, 339–341. https://doi.org/10.1107/S0108767307043930.

Sheldrick, G.M., 2015. ShelXT-Integrated space-group and crystal-structure determination. Acta Crystallogr. A71, 3–8. https://doi.org/10.1107/S2053273314026370.

Wang, X., Jin, X.Y., Zhou, J.C., Zhu, R.X., Qiao, Y.N., Zhang, J.Z., Li, Y., Zhang, C.Y., Chen, W., Chang, W.Q., Lou, H.X., 2020. Terpenoids from the Chinese liverwort *Heteroscyphus coalitus* and their antivirulence activity against *Candida albicans*. Phytochemistry 174, 112324. https://doi.org/10.1016/j.phytochem.2020.112324.

Wee, S., Carroll, F.I., Woolverton, W.L., 2006. A reduced rate of in vivo dopamine transporter binding is associated with lower relative reinforcing efficacy of stimulants. Neuropsychopharmacology 31, 351–362. https://doi.org/10.1038/sj.npp.1300795.

Zhao, L., Johnson, K.M., Zhang, M., Flippen-Anderson, J., Kozikowski, A.P., 2000. Chemical synthesis and pharmacology of 6- and 7-hydroxylated 2-carbomethoxy-3-(*p*-tolyl) tropanes: Antagonism of cocaine's locomotor stimulant effects. Med. Chem. 43, 3283–3294. https://pubs.acs.org/doi/10.1021/jm000141b.